

Abstract

There is growing evidence in favour of the temporal-coding hypothesis that temporal correlation of neuronal discharges may serve to bind distributed neuronal activity into unique representations and, in particular, that θ (3.5-7.5 Hz) and δ (0.5 < 3.5 Hz) oscillations facilitate information coding. The θ and δ rhythms are shown to be involved in various sleep stages, and during anaesthesia, and they undergo changes with the depth of anaesthesia. We introduce a thalamocortical model of interacting neuronal ensembles to describe phase relationships between θ and δ oscillations, especially during deep and light anaesthesia. Asymmetric and long range interactions among the thalamocortical neuronal oscillators are taken into account. The model results are compared with the experimental observations of Musizza et al. *J. Physiol. (London)* 2007 580:315-326. The δ and θ activities are found to be separately generated and are governed by the thalamus and cortex respectively. Changes in the degree of intra-ensemble and inter-ensemble synchrony imply that the neuronal ensembles inhibit information coding during deep anaesthesia and facilitate it during light anaesthesia.

Neuronal synchrony during anaesthesia - A thalamocortical model

Jane H. Sheeba
Department of Physics,
Lancaster University,
Lancaster, LA1 4YB, UK

Aneta Stefanovska ¹
Department of Physics,
Lancaster University,
Lancaster, LA1 4YB, UK

Peter V. E. McClintock
Department of Physics,
Lancaster University,
Lancaster, LA1 4YB, UK

November 21, 2021

¹Department of Physics, Lancaster University, Lancaster, LA1 4YB, UK

1 Introduction

Neuronal communication and synchronization are crucially important features of the co-operative interaction between neuronal ensembles, endowing the brain with the marvelous capability known as *cognition*. The time scales of human motor and cognitive events are comparable to that of the EEG field dynamics arising from synchronous activity, observable from within or outside the brain (1). Since EEG signals correspond to the averaged activity of large cell populations, their fluctuations can support cognitive activity only if they are sufficiently synchronized: effective communication of neuronal ensembles can be achieved only if they are oscillating in a synchronized manner. Such behavior tags those neurons to represent particular cognitive tasks, e.g. in relation to a perceptual object (2).

In this article we present a model of interacting thalamocortical neuronal ensembles in an attempt to account for the behaviour of δ and θ waves during anaesthesia. Our model is motivated by an attempt to tackle the problem of anaesthetic awareness, to provide the basic understanding needed to prevent people inadvertently awakening during surgery. We therefore focus on ways to identify and characterize the states of deep and light anaesthesia. Our starting point model is the experimental observation that both the cardio-respiratory and respiratory- δ interactions change with depth of anaesthesia in rats (3, 4) following the administration of a single bolus of ketamine-xylazine. During the ensuing deep phase of anaesthesia (~ 45 min) the amplitude of δ -waves is strongly pronounced. As the subsequent light phase of anaesthesia (~ 25 min) is entered, the δ -waves disappear and the amplitude of θ -waves increases. We use the phase dynamics approach to propose a model that incorporates regional ensembles of neurons that are connected both among and between themselves.

Further, we investigate the role played by the neuronal ensembles in temporal coding during deep and light anaesthesia from the model results. Neuronal synchrony is often associated with an oscillatory pattern of signals (oscillation-based synchrony). The frequencies of such signals generally cover a broad range and, more importantly, exhibit a marked state dependence. In other words, synchrony and temporal coding of information in selective frequency bands are two different sides of the same coin. We use this idea and establish the link between the conditions under which temporal coding is believed to occur (synchrony) and the level of arousal of the brain.

1.1 Physiological background

During periods of slow wave sleep/anæsthesia, widespread synchronized oscillations occur throughout the thalamus and the cortex. The slow oscillations ($< 1\text{Hz}$) that occur during natural sleep and ketamine–xylazine anæsthesia are an emergent network property of neocortical neurons involving the TC and RE neurons (5). The clock-like δ ($1 - 4\text{Hz}$) are produced in the thalamus and are strongly synchronized by the RE and the thalamocortical volleys (6). A small proportion of the TC neurons also display slow and δ oscillations (5). Thus the high amplitude, low frequency δ and slow oscillations are found to be associated with highly coherent activities of the cortical, RE and TC neurons. The dynamics of δ and θ waves can therefore be represented by interacting ensembles of neuronal oscillators.

The physiological circuitry is as shown in Fig. 1 (left) (7). The pyramidal (PY) neurons of the cerebral cortex are connected among themselves (excitatory) by the interneurons (IN) which also form components of the cortical ensemble. The TC neurons receive sensory inputs which are relayed to the appropriate area of the cortex through ascending thalamocortical fibres (indicated by the upward arrow). The RE neurons wrap most of the dorsal and ventral aspects of thalamus (8) and act as bridge between the TC neurons and the thalamic neurons. The dense axons of the RE neurons innervate the TC neurons (9). The corticothalamic fibers (indicated by the downward arrow) also leave collaterals within the RE nucleus and dorsal thalamus. The RE neurons thus form a network that surrounds the thalamus. It receives a copy of nearly all thalamocortical and corticothalamic activity, and projects connections *solely* to neurons in the TC region (7). In turn, the axons of the TC neurons give rise to collaterals in the RE nucleus while the parent axon passes through the cerebral cortex (10).

2 The model

Based on the physiological phenomena that take place during anæsthesia, as well as on anatomy, the model system considered is shown schematically in Fig. 1 (right). The oscillators in the three ensembles, namely the cortical, the thalamic reticular and the thalamocortical relay neurons, have different mean natural frequencies and their interactions are characterized by intrapopulation and inter-population coupling parameters.

Each neuron in the ensembles is considered as an oscillator whose membrane potential is the oscillating variable. The couplings represent the synaptic connections between them. We reduce the system to a phase model,

one of the simplest yet accurate models for weakly coupled nonlinear oscillators, with the coupling being introduced through the phases. In doing so, we make use of the fact that there exists a degree of coherence between the membrane potential oscillations and the action potential firings. Although they are not equivalent, the action potentials are triggered at a certain phase of the membrane potential oscillations. This reasoning leads to the following set of equations

$$\begin{aligned}
\dot{\theta}_i^{(1)} &= \omega_i^{(1)} - \frac{A_c}{N} \sum_{j=1}^N \sin(\theta_i^{(1)} - \theta_j^{(1)} + \alpha) \\
&\quad - \frac{B_c}{N} \sum_{j=1}^N \sin(\theta_i^{(1)} - \theta_j^{(2)} + \alpha) + \eta_i^{(1)}, \\
\dot{\theta}_i^{(2)} &= \omega_i^{(2)} - \frac{A_{tc}}{N} \sum_{j=1}^N \sin(\theta_i^{(2)} - \theta_j^{(2)} + \alpha) \\
&\quad - \frac{B_{tc}}{N} \sum_{j=1}^N \sin(\theta_i^{(2)} - \theta_j^{(1)} + \alpha) \\
&\quad - \frac{C_{tc}}{N} \sum_{j=1}^N \sin(\theta_i^{(2)} - \theta_j^{(3)} + \alpha) + \eta_i^{(2)}, \\
\dot{\theta}_i^{(3)} &= \omega_i^{(3)} - \frac{A_{re}}{N} \sum_{j=1}^N \sin(\theta_i^{(3)} - \theta_j^{(3)} + \alpha) \\
&\quad - \frac{B_{re}}{N} \sum_{j=1}^N \sin(\theta_i^{(3)} - \theta_j^{(2)} + \alpha) + \eta_i^{(3)},
\end{aligned} \tag{1}$$

where $\theta_i^{(1,2,3)}$ are the phases of the i th oscillator in the C, TC and RE ensembles, respectively, and N refers to the ensemble sizes. The parameters A_c , A_{tc} and A_{re} quantify intra-ensemble couplings and B_c , B_{tc} , C_{tc} and B_{re} quantify the inter-ensemble couplings. The natural oscillator frequencies $\omega_i^{(1,2,3)}$ are assumed to be distributed with central frequencies $\bar{\omega}^{1,2,3}$. The $\eta_i^{(1,2,3)}$ are independent white Gaussian noises for which $\langle \eta_i^{(1,2,3)}(t) \rangle = 0$ and $\langle \eta_i^{(1,2,3)}(t) \eta_j^{(1,2,3)'}(t') \rangle = 2D_{(1,2,3)} \delta(t - t') \delta_{ij}$; $D_{(1,2,3)}$ are the noise intensities. For convenience one can define complex-valued, mean field, order parameters as $r_{(1,2,3)} e^{i\psi_{(1,2,3)}} = \frac{1}{N} \sum_{j=1}^N e^{i\theta_j^{(1,2,3)}}$. Here $\psi_{1,2,3}(t)$ are the average phases of the oscillators in the respective ensembles and $r_{1,2,3}(t)$ are measures of the

coherence of the oscillator ensembles, which vary from 0 to 1. With these definitions, Eqs. (1) become

$$\begin{aligned}
\dot{\theta}_i^{(1)} &= \omega_i^{(1)} - r_1 A_c \sin(\theta_i^{(1)} - \psi_1 + \alpha) \\
&\quad - r_2 B_c \sin(\theta_i^{(1)} - \psi_2 + \alpha) + \eta_i^{(1)}, \\
\dot{\theta}_i^{(2)} &= \omega_i^{(2)} - r_2 A_{tc} \sin(\theta_i^{(2)} - \psi_2 + \alpha) \\
&\quad - r_1 B_{tc} \sin(\theta_i^{(2)} - \psi_1 + \alpha) \\
&\quad - r_3 C_{tc} \sin(\theta_i^{(2)} - \psi_3 + \alpha) + \eta_i^{(2)}, \\
\dot{\theta}_i^{(3)} &= \omega_i^{(3)} - r_3 A_{re} \sin(\theta_i^{(3)} - \psi_3 + \alpha) \\
&\quad - r_2 B_{re} \sin(\theta_i^{(3)} - \psi_2 + \alpha) + \eta_i^{(3)}.
\end{aligned} \tag{2}$$

2.1 Numerical methods

A fourth-order Runge-Kutta routine is used for the numerical simulation with the initial phases equally distributed within $[0, 2\pi]$. The results are normalized to “real time” and the system is simulated for the equivalent of 60 mins with $N = 10000$. We will refer to synchrony within an ensemble as *intra-ensemble synchrony*, and that between ensembles as *inter-ensemble synchrony*. The amount of intra-ensemble synchrony is measured by the mean field parameters: $r_{(1,2,3)} = 0$ implies that there is no synchrony in the corresponding ensemble; $r_{(1,2,3)} = 1$ indicates complete synchrony; and $0 < r_{(1,2,3)} < 1$ corresponds to partial synchrony. The greater the value of $r_{(1,2,3)}$, the more oscillators are oscillating in synchrony (11, 12). On the other hand, inter-ensemble synchrony occurs when oscillators from two different ensembles entrain to a frequency/phase window. In general, inter-ensemble synchrony can be quantified by a constant difference in the mean phases $\psi_{(1,2,3)}$. However, this measurement will be valid only if both the ensembles are completely locked to each other. For partial synchrony, the difference in the mean phase will be oscillating, showing no synchrony. Hence we identify inter-ensemble synchrony by looking at the time evolution of the ensemble-averaged frequencies. Also, for increasing inter-ensemble coupling parameters, a decrease in $r_{(1,2,3)}$ is a signature of inter-ensemble synchrony (13).

The inter-ensemble and intra-ensemble coupling parameters are swept linearly in time in order to mimic the effect of decreasing concentration of anaesthetic agent. This corresponds to the ability of anaesthetics to affect thalamocortical signalling, as is well recognized from *in vivo* electrophysio-

logical work on animals (14). Thus, during deep anæsthesia, the neuronal oscillators are very weakly coupled so that they do not interact much (due to the anæsthetics blocking the signalling pathways). As the anæsthetic concentration wears off the signalling pathways become unblocked and the couplings between the neuronal oscillators and ensembles become stronger. Hence we can simulate the transition from the deeply to the lightly anæsthetized state by starting with a very weak coupling strength (characterizing deep anæsthesia) and continuously sweeping them to stronger values with time. The starting values of the coupling parameters are given in Fig. 2. We introduce asymmetry in the model by a phase shift $0 \leq \alpha < \pi/2$. For the values of the mean frequencies we follow Amzica et al. (15, 16); $\bar{\omega}^{(1)} = 3$ Hz, $\bar{\omega}^{(2)} = 1.5$ Hz and $\bar{\omega}^{(3)} = 1$ Hz, with Lorentzian distributions $g(\omega^{(1,2,3)}) = \frac{\gamma}{\pi}(\gamma^2 + (\omega - \bar{\omega}^{(1,2,3)})^2)^{-1}$.

Our choice of values for the mean frequencies reflects the intrinsic properties of the neurons. The cortical neurons are endowed with intrinsic properties which could be reflected in field potential recordings as δ activities. The frequencies of these faster oscillations evolve around the upper limit of the delta band (mainly 3–4 Hz) (15, 16, 17). The clock-like δ oscillations (1–4 Hz) are mainly produced in the RE neurons (5). Individual TC neurons are capable of producing Ca^{2+} spikes and associated action potentials at frequencies of 0.5–4 Hz (6).

3 Results

The time evolution of the mean frequency of each ensemble is plotted in Fig. 2 right. For comparison, the experimental δ and θ frequencies, obtained by wavelet analysis of the EEG signals from anæsthetised rats (3), are plotted in Fig. 2 (left). In the latter experiments, the δ activity was found initially to be of higher amplitude compared to that of the θ waves. In particular, during the deep phase of anæsthesia, there occurs a strong, high amplitude, δ activity which greatly diminishes on entry to the light phase (at ~ 45 min). The θ activity runs independently throughout the whole period of anæsthesia, but at a much lower amplitude compared to that of the δ waves. Note the differences in the amplitudes corresponding to the color codes in Fig. 2 left, which makes the θ activity visible in the top panel.

The model results suggest that it is the TC and RE ensembles that generate the δ activity during deep anæsthesia. This δ is of high amplitude due to the strong synchrony in and between the TC and RE ensembles. Synchrony between the TC and RE ensembles can be easily established even

with a smaller value of inter-ensemble coupling, because the frequency difference between them is relatively small. Fig. 3 shows the time evolutions of the mean field parameters $r_{(1,2,3)}$ of the three ensembles corresponding to the simulated frequencies. During deep anaesthesia, the fractions of oscillators that oscillate in synchrony in the TC and RE ensembles are higher than in the C ensemble. This results in a strongly pronounced δ while the amplitude of θ remains low due to very low number of oscillators oscillating in synchrony in the C ensemble (see Fig. 3).

On the other hand, for the thalamus (TC+RE) to be synchronized with the cortex, a relatively higher value of coupling strength is required. This occurs at ~ 45 min, at which point the TC and RE frequencies shift to a higher value to join the C ensemble and produce θ activity. This is the reason for the sudden diminution of the δ and appearance of θ at ~ 45 min. Of course, the exact time of occurrence depends on the value of the coupling parameter that we choose. As a consequence of the shift (inter-ensemble synchrony), the amount of intra-ensemble synchrony is reduced in the TC and RE ensembles (13) and hence the θ appears as a low-amplitude activity. We thus quantify the amplitudes of the characteristic δ and θ activities by the mean field parameters $r_{(1,2,3)}$ which reveals the amount of synchrony in each ensemble and hence the amplitude of the oscillations. The intra-ensemble and inter-ensemble synchronisation mechanisms discussed here are generic to systems of coupled oscillator ensembles (11, 12, 13, 18, 19, 20, 21, 22, 23).

3.1 Phase coding and depth of anaesthesia

The δ and θ phases play significant roles in coding information when the brain is not in an aroused state, characterized by desynchronized EEG. The level with which the phases are synchronized determines the ability to code information. However, it is the inter-ensemble synchrony that plays the crucial role in temporal binding (rather than the intra-ensemble synchrony). Since synchrony is supposed to enhance the significance of responses of the neurons (2), it is obvious that synchronized discharges will have a stronger impact than temporally disorganized ones (24). Thus the θ phase is found to play a crucial role in inhibiting information by being poorly synchronized in the cortex. More importantly though, the cortex and the thalamus are not in synchrony with each other (see Fig. 3). Due to this, binding of information cannot be achieved, which is why consciousness and cognition are absent during the deep phase of anaesthesia. The strong δ waves keep the cortex and the thalamus out of phase with each other during deep anaesthesia.

On the other hand, the thalamus enters into synchrony with the cortex on emergence from anaesthesia. This corresponds to the state of awareness when information can be successfully coded due to the emergence of inter-ensemble synchrony, characterized by the θ phase (see Figs. 2 and 3).

4 Discussion

The model results indicate that the δ and the θ activities observed experimentally are separate in terms of their generation and frequency. The δ and θ activities are found to occur mainly in 0.5 – 3.5 Hz and 3.5 – 7.5 Hz bands in agreement with recent observations (3) and earlier reports (15, 16). The dramatic diminution of the δ amplitude and the simultaneous appearance of θ activity characterize the transition from deep to light anaesthesia.

In the experiment (3), the amplitudes of the δ and θ waves differed by more than a factor of 10. In order to reveal θ (which otherwise would have been lost in the noise level of δ) two separate figures were therefore plotted with different amplitude scales. Our model results suggest that θ activity is present during both deep and light anaesthesia. However, during deep anaesthesia the δ activity is highly synchronized, whereas θ activity is poorly synchronized (see Fig. 3). The effect on their relative amplitudes is that the θ activity cannot be seen during the deep anaesthesia in the experiment, consistent with the observations, despite its presence as revealed by the model.

Although varying the coupling parameters to mimic the effect of decreasing concentration of the anaesthetic agent helps us to understand and compare the model results with reality, it introduces oscillations in the frequencies. As is evident from Fig. 2, the mean frequencies of each of the ensembles undergo noisy oscillations, while remaining within the δ/θ bands. The effect of varying coupling parameters affects the frequencies directly because the model equations are for the oscillator phases and the frequencies are calculated from the phases themselves. Likewise, the oscillations seen in the order parameters (Fig. 3) are introduced mainly by the change in inter-ensemble coupling parameters.

Since the model considers only the phases, and not the amplitudes, we are unable to make a direct comparison with the experimental results. However, we make use of the theory of synchronization to quantify the amplitude in terms of the amount of synchrony in each of the ensembles. That is, the more the synchrony, the more oscillators are oscillating in phase with each other, and hence the higher the corresponding oscillation amplitude. On the

other hand, the model does offer the advantage that we are able to identify those neuronal groups that are responsible for the generation of δ and θ activity during anaesthesia.

Although we do not challenge the importance of the microscopic details underlying general anaesthesia and the Hodgkin-Huxley formalisms (25), the model results support the hypothesis that consideration of macroscopic dynamics with asymmetry is important. We therefore suggest that models of similar kinds can be used to explain experimental observations, not only in anaesthesia, as here, but also in other cognitive and behavioral states that involve huge numbers of neurons functioning in groups. Detailed work has been done in the field of neuronal mass modeling and a wide range of EEG generative models have been proposed (26, 27, 28, 29, 30, 31, 32). Our model is capable of generating the wide range of EEG oscillatory behaviors reported earlier (33, 34, 35, 36, 37). Our findings uniquely identify the link between neuronal synchrony and temporal coding especially in terms of inter-ensemble synchrony. An additional advantage of the model is that it yields insight into the synchronization mechanisms underlying the δ and θ waves.

5 Conclusion

In summary, we have introduced a model involving asymmetrically interacting ensembles of C, TC and RE neurons in order to understand the mechanisms underlying the generation of δ and θ waves during anaesthesia. The model results are compared with those from experiments (3). The TC and the RE ensembles were found to be responsible for the generation of high amplitude δ waves during deep anaesthesia. The C ensemble is engaged with the θ activity. The transition from deep to light anaesthesia is found to be marked by a frequency shift in the TC and RE ensembles, caused by the increase in the coupling strengths. Also, the θ activity is found not to be as strongly synchronized as the δ activity. The similarities and differences between the model results and the experimental results were discussed. Furthermore, the model illuminates the phenomenon of temporal coding of information, in particular by the δ and θ frequencies. It reveals the role played by the neuronal phases in inhibiting information during deep anaesthesia and coding the sensory information during light anaesthesia. Although our main motivation for introducing the model was to understand the mechanisms giving rise to the generation of δ and θ waves during ketamine-xylazine anaesthesia in rats (3, 4), it can also be used to elucidate the mechanisms in-

volved in the generation of brain waves for other anaesthetics and also during slow wave sleep. The results derived from the model will have implications for the understanding of fMRI and MEG dynamics.

The study was supported by the EC FP6 NEST-Pathfinder project BRACCIA and in part by the Slovenian Research Agency.

References

1. Del Negro, C. A., C. G. Wilson, R. J. Butera, H. Rigatto, and J. C. Smith. 1999. Periodicity, mixed-mode oscillations, and quasiperiodicity in a rhythm-generating neural network. *Biophys. J.* 24:206-214.
2. Singer, W. 1999. Neuronal synchrony: A versatile code for the definition of relations? *Neuron* 24:49-65.
3. Musizza, B., A. Stefanovska, P. V. E. McClintock, M. Palus, J. Petrovcic, S. Ribaric, and F. F. Bajrovic. 2007. Interactions between cardiac, respiratory and EEG-delta oscillations in rats during anaesthesia. *J. Physiol. (London)* 580:315-326.
4. Stefanovska, A., H. Haken, P. V. E. McClintock, M. Hoic, F. Bajrovic, and S. Ribaric. 2000. Reversible transitions between synchronization states of the cardiorespiratory system. *Phys. Rev. Lett.* 85:4831-4834.
5. Contreras, D., and M. Steriade. 1997. Synchronization of low-frequency rhythms in corticothalamic networks. *Neuroscience* 76:11-24.
6. Bal, T., and D. A. McCormick. 1996. What stops synchronized thalamocortical oscillations? *Neuron* 17:297-308.
7. Destexhe, A., and T. J. Sejnowski. 2003. Interactions between membrane conductances underlying thalamocortical slow-wave oscillations. *Physiol. Rev.* 83:1401-1453.
8. Jones, E. G. 1985. *The Thalamus*. Plenum, New York.
9. Cox, C. L., J. R. Huguenard, and D. A. Prince. 1996. Heterogeneous axonal arborizations of rat thalamic reticular neurons in the ventrobasal nucleus. *J. Comp. Neurol.* 366:416-430 .
10. Harris, R. M. 1987. Axon collaterals in the thalamic reticular nucleus from thalamocortical neurons of the rat ventrobasal thalamus. *J. Comp. Neurol.* 258:397-406.

11. Kuramoto, Y. 1984. *Chemical Oscillations, Waves, and Turbulence*. Springer-Verlag, Berlin.
12. Pikovsky, A., M. Rosenblum, and J. Kurths. 2001. *Synchronization – A Universal Concept in Nonlinear Sciences*. Cambridge University Press, Cambridge.
13. Jane H. Sheeba, V. K. Chandrasekar, A. Stefanovska, and P. V. E McClintock. 2008. Routes to synchrony between asymmetrically interacting oscillator ensembles. (in preparation).
14. Alkire, M. T., R. J. Haier, and J. H. Fallon. 2000. Toward a unified theory of narcosis: Brain imaging evidence for a thalamocortical switch as the neurophysiologic basis of anesthetic-induced unconsciousness. *Conscious Cogn.* 9:370-386.
15. Amzica, F. 2002. In vivo electrophysiological evidences for cortical neuron-glia interactions during slow (< 1 Hz) and paroxysmal sleep. *J. Physiol. (Paris)* 96:209-219.
16. Amzica, F., and M. Steriade. 1998. Electrophysiological correlates of sleep δ waves. *Electroenceph. and Clinical Neurophysiol.* 107:69-83.
17. Steriade, M. 2006. Grouping of brain rhythms in corticothalamic systems. *Neuroscience* 137:1087-1106.
18. Winfree, A. T. 1980. *The Geometry of Biological Time*. Springer-Verlag, New York.
19. Okuda, K., and Y. Kuramoto. 1991. Mutual entrainment between populations of coupled oscillators. *Prog. Theor. Phys.* 86:1159-1176.
20. Strogatz, S. H. 2000. From Kuramoto to Crawford: exploring the onset of synchronization in populations of coupled oscillators. *Physica D* 143:120.
21. Montbrió, E., J. Kurths, and B. Blasius. 2004. Synchronization of two interacting populations of oscillators. *Phys. Rev. E* 70:056125.
22. Daido, H., and K. Nakanishi. 2006. Diffusion-induced inhomogeneity in globally coupled oscillators: Swing-by mechanism. *Phys. Rev. Lett.* 96:054101.

23. Kiss, I. Z., M. Quigg, S. H. C. Chun, H. Kori, and J. L. Hudson. 2008. Characterization of synchronization in interacting groups of oscillators: Application to seizures. *Biophys. J.* 94:1121-1130.
24. Alonso, J. M., W. M. Usrey, and R. C. Reid. 1996. Precisely correlated firing in cells of the lateral geniculate nucleus. *Nature* 383:815-819.
25. Hodgkin, A. L., A. F. Huxley, and B. Katz. 1949. Ionic currents underlying activity in the giant axon of the squid. *Arch. Sci. physiol.* 3:129-150.
26. Wilson, H. R. and J. D. Cowan. 1972. Excitatory and inhibitory interactions in localized populations of model neurons. *Biophys. J.* 12:124.
27. Nunez, P. 1974. The brain wave equation: a model for the EEG. *Math. Biosci.* 21:279.
28. Lopes da Silva, F. H., A. van Rotterdam, P. Barts, E. van Heusden, and W. Burr. 1976. Models of neuronal populations: the basic mechanisms of rhythmicity. *Prog. Brain Res.* 45:281308.
29. Freeman, W. J. 1978. Models of the dynamics of neural populations. *Electroencephalogr. Clin. Neurophysiol.* Suppl.:918.
30. Jansen, B. H., and V. G. Rit. 1995. Electroencephalogram and visual evoked potential generation in a mathematical model of coupled cortical columns. *Biol. Cybern.* 73:357366.
31. Valdes, P. A., J. C. Jimenez, J. Riera, R. Biscay, and T. Ozaki. 1999. Nonlinear EEG analysis based on a neural mass model. *Biol. Cybern.* 81:415424.
32. David, O., and K. J. Friston. 2003. A neural mass model for MEG/EEG: coupling and neuronal dynamics. *NeuroImage* 20:17431755.
33. Jirsa, V. K., and H. Haken. 1996. Field theory of electromagnetic brain activity. *Phys. Rev. Lett.* 77:960963.
34. Wright, J. J., P. A. Robinson, C. J. Rennie, E. Gordon, P. D. Bourke, C. L. Chapman, N. Hawthorn, G. J. Lees, and D. Alexander. 2001. Toward an integrated continuum model of cerebral dynamics: the cerebral rhythms, synchronous oscillation and cortical stability. *Biosystems* 63:7188.

35. Wright, J. J., C. J. Rennie, G. J. Lees, P. A. Robinson, P.D. Bourke, C. L. Chapman, E. Gordon, and D. L. Rowe. 2003. Simulated electrocortical activity at microscopic, mesoscopic, and global scales. *Neuropsychopharmacology* 28 (Suppl. 1):S80S93.
36. Rennie, C. J., P. A. Robinson, and J. J. Wright. 2002. Unified neurophysical model of EEG spectra and evoked potentials. *Biol. Cybern.* 86:457471.
37. Robinson, P. A., C. J. Rennie, D. L. Rowe, S. C. OConnor, J. J. Wright, E. Gordon, and R. W. Whitehouse. 2003 Neurophysical modeling of brain dynamics. *Neuropsychopharmacology* 28(Suppl. 1):S74S79.

Figure Legends

Figure 1.

Left – The arrangements and connectivity of four types of cells, namely the TC, RE, C (comprised of the IN and PY cells). Pre refers to external pre-thalamic afferent sensory inputs. The upward and downward arrows represent the thalamocortical and corticothalamic fibres respectively. After (7), with permission. Right – Schematic representation of the model. There are three ensembles: cortical neurons(C), thalamocortical relay neurons (TC), and thalamic reticular neurons (RE). They interact both among themselves (represented by the circle in each case) and between each other (represented by the arrows). The upward and the downward arrows indicate the thalamocortical and corticothalamic connections. External afferent (pre-thalamic) inputs to the thalamus are denoted as Pre.

Figure 2.

Left – The time evolution of the characteristic EEG δ and θ frequencies during Ketamine–xylazine anaesthesia, analyzed by wavelet transform. Reproduced from (3), with permission. Right – The time evolution of the characteristic δ and θ frequencies displayed by three ensembles C (blue), TC (red) and RE (green), as obtained from the model. The (starting) values of the (coupling) parameters were $A_c = 0.8$, $B_c = 1.2$, $A_{tc} = 0.9$, $B_{tc} = 0.45$, $C_{tc} = 0.9$, $A_{re} = 0.2$, $B_{re} = 0.65$, $\alpha = 0.9$, $D_1 = 0.1$, $D_2 = 0.2$, $D_3 = 0.15$ and $\gamma = 0.4$.

Figure 3.

Mean field parameters $r_{(1,2,3)}$ of the three ensembles, plotted as functions of time, corresponding to the frequencies plotted in Fig. 2 (right) for the same values of parameters.

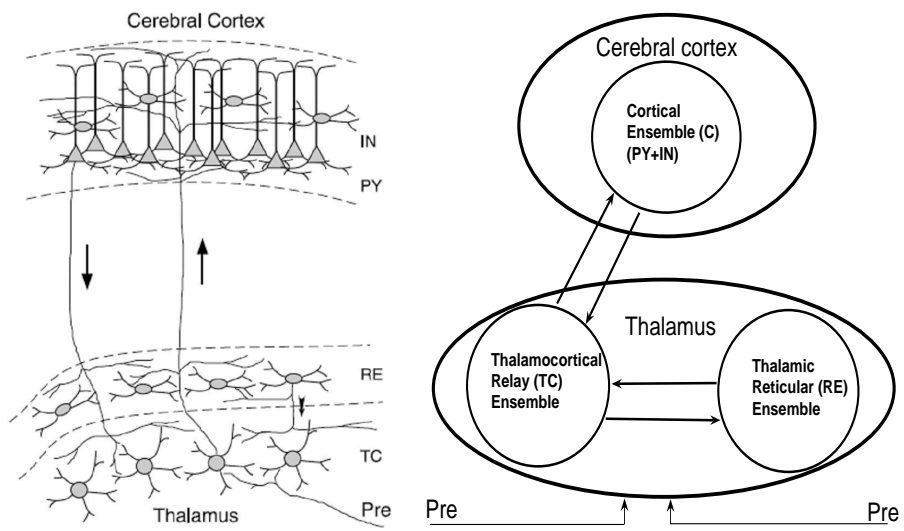


Figure 1:

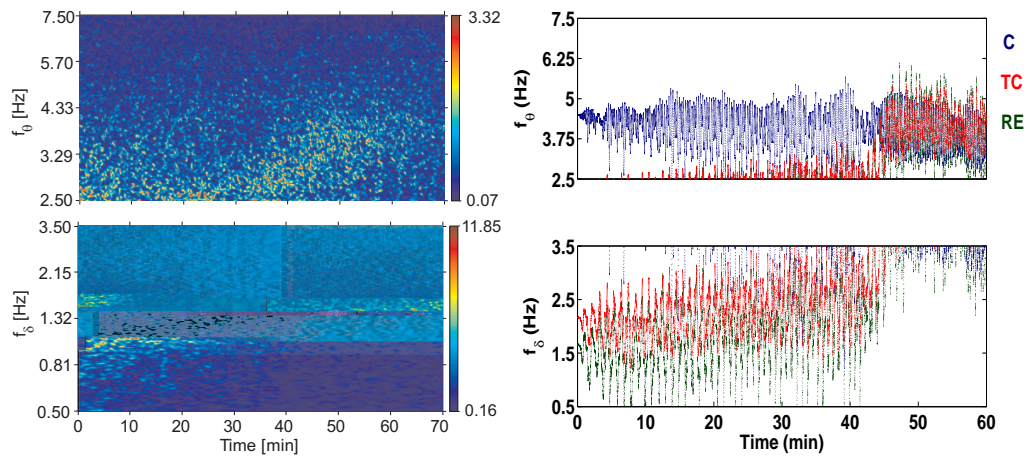


Figure 2:

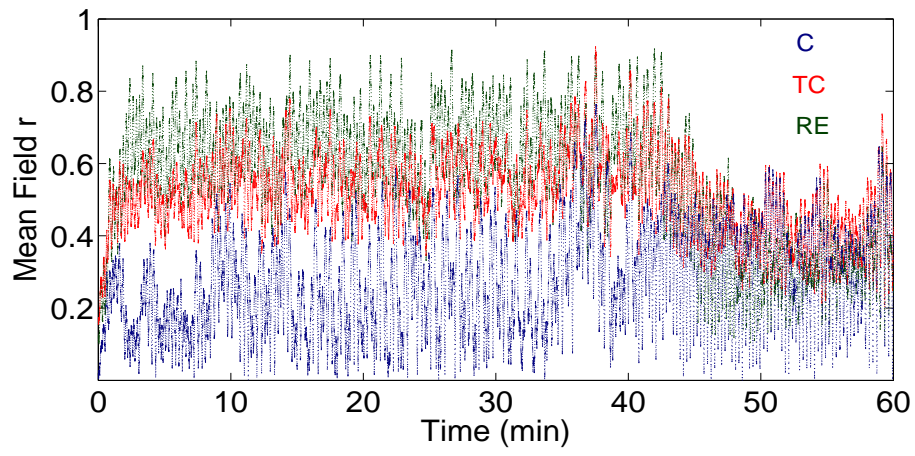


Figure 3: